Proceedings of the 1st Global Power and Propulsion Forum
GPPF 2017
Jan 16-18, 2014, Zurich, Switzerland
www.pps.global

GPPF-2017-42

PROPOSAL AND VALIDATION OF A SIMPLE MODEL FOR MEAN DIAMETER AND SIZE DISTRIBUTION BY LIQUID SHEET ATOMIZATION

Chihiro Inoue
The University of Tokyo
inoue@rocketlab.t.u-tokyo.ac.jp
Tokyo, Japan

Toshinori Watanabe
The University of Tokyo
watanabe@aero.t.u-tokyo.ac.jp
Tokyo, Japan

Takehiro Himeno
The University of Tokyo
himeno@aero.t.u-tokyo.ac.jp
Tokyo, Japan

Seiji Uzawa
The University of Tokyo
uzawa@aero.t.u-tokyo.ac.jp
Tokyo, Japan

ABSTRACT

We expect to provide an instantaneous estimation methodology of droplet size for a design of spray nozzles. Here we perform a simple and fundamental theoretical analysis on atomization of an axisymmetric liquid sheet as in a disk atomizer. The theoretical model is derived based on the energy conservation law assuming several reasonable hypotheses. We derive an equation of Sauter mean diameter (SMD), which is inversely proportional to the injection Weber number under turbulent condition. A non-dimensional exponential distribution function is also obtained from the formulated SMD without using fitting parameters. The new framework is favorably validated by comparing with experimental values. A corresponding numerical simulation of free surface flow convinces the mechanism of an energy conversion process, which supports the idea of the theoretical model

INTRODUCTION

It is convenient to predict spray characteristics in advance for a design of desirable spray nozzles to inject fuel and water introduced in gas turbines. One of the most important characteristics is droplet diameters. There have been many attempts to predict mean droplet diameters [1]-[4] and their distributions [5]-[11]. Empirical correlations for mean diameters are proposed for various types of nozzles [1][2]. Theoretical methods [3][4] derived in the past use several experimental parameters, which are determined by experimental measurements. For example, a method [3] based on a linear stability analysis requires an empirical constant relating to the initial amplitude of disturbance. As a result, it is difficult to predict droplet diameters when the shape of the injector is modified or the properties of the working liquid are changed. Empirical distribution functions are also proposed [5]-[7]. Maximum Entropy Formalism [8][9], one of theoretical methods, is able to estimate droplet size distributions if some mean diameters are already provided. Discrete Probability Function (DPF) approach [10][11] requires fluctuation quantities, which are difficult to be determined. Recently, numerical simulations have been carried out to calculate droplet diameters, e.g. stochastic breakup models [12][13], Eulerian approach [14][15] or Eurelian/Lagrangian hybrid approach [16]-[18]. In usual, however, their results are highly dependent on grid resolutions, and it takes long time to accumulate a sufficient number of droplets for calculating mean diameters and size distributions. Therefore, even though empirical methods, theoretical models, and CFD based calculations have been widely utilized, it is still difficult to estimate instantaneously the mean diameters and the size distributions in a new nozzle or at a different condition. We expect a convenient model is useful at an early design stage, which requires no experimental parameters and little time to calculate, and provides reasonable degree of accuracy. Authors proposed such method in the past based on the energy conservation law [19][20]. However, the distribution functions contained fitting parameters,

In the present study, an estimation method both for mean droplet diameter and size distribution is consistently proposed. The feature is that it does not need experimental parameters. It is expected to provide an evidence for instantaneous design decisions and modifications. From a fundamental point of view, we produce and analyse an axisymmetric liquid sheet by impinging a liquid jet on a small circular disk.

In the following, first, the energy conservation law for the atomization phenomenon is generally described and

simplified with various reasonable assumptions. Second, an estimation method for SMD and droplet size distribution is derived. Third, calculated results are compared with corresponding experimental results. Finally, an energy conversion process following the energy conservation law is demonstrated by a numerical simulation.

ENERGY CONSERVATION LAW FOR ATOMIZATION

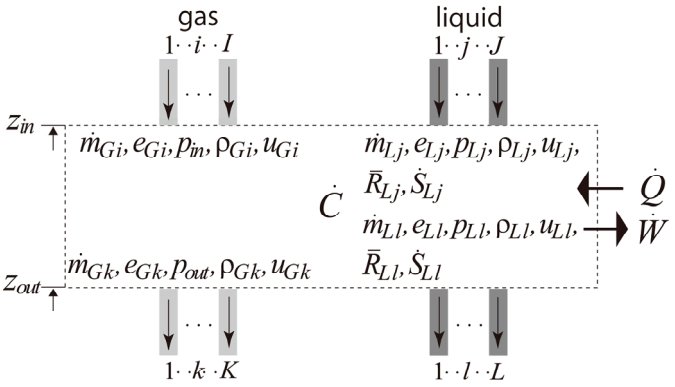

Fig.1 Control volume [19]

Figure 1 shows the control volume, where liquid and gas flow in and out. Equation (1) represents the energy conservation law.

$$\begin{aligned}\dot{Q}-\dot{W}+\dot{C}=&\sum_i \dot{m}_{Gi}\left[e_{Gi}+\frac{p_{in}}{\rho_{Gi}}+\frac{1}{2}u_{Gi}^2+gz_{in}\right]\\&+\sum_j \dot{m}_{Lj}\left[e_{Lj}+\frac{p_{Lj}}{\rho_{Lj}}+\frac{1}{2}u_{Lj}^2+gz_{in}\right]\\&+\sum_j \sigma_{Lj}\dot{S}_{Lj}\\&-\sum_k \dot{m}_{Gk}\left[e_{Gk}+\frac{p_{out}}{\rho_{Gk}}+\frac{1}{2}u_{Gk}^2+gz_{out}\right]\\&-\sum_l \dot{m}_{Ll}\left[e_{Ll}+\frac{p_{Ll}}{\rho_{Ll}}+\frac{1}{2}u_{Ll}^2+gz_{out}\right]\\&-\sum_l \sigma_{Ll}\dot{S}_{Ll}\end{aligned} \tag{1}$$

On the right hand side, the fluid energy consists of the total enthalpy, the potential energy, and the liquid surface free energy. The pressure inside the liquid is higher than the ambient gas by an amount equal to the Laplace pressure, which is proportional to the averaged curvature.

$$p_{Lj}=p_{in}+2\sigma_{Lj}/\bar{R}_{Lj} \tag{2}$$

$$p_{Ll}=p_{out}+2\sigma_{Ll}/\bar{R}_{Ll}\,. \tag{3}$$

Equation (4) below is derived by substituting Eqs.(2) and (3) into Eq.(1).

$$\begin{aligned}&\sum_l \sigma_{Ll}\left(\frac{2\dot{m}_{Ll}}{\rho_{Ll}\bar{R}_{Ll}}+\dot{S}_{Ll}\right)-\sum_j \sigma_{Lj}\left(\frac{2\dot{m}_{Lj}}{\rho_{Lj}\bar{R}_{Lj}}+\dot{S}_{Lj}\right)\\&=-(\dot{Q}-\dot{W}+\dot{C})\\&+\sum_i \dot{m}_{Gi}\left[e_{Gi}+\frac{p_{in}}{\rho_{Gi}}+\frac{1}{2}u_{Gi}^2+gz_{in}\right]+\sum_j \dot{m}_{Lj}\left[e_{Lj}+\frac{p_{in}}{\rho_{Lj}}+\frac{1}{2}u_{Lj}^2+gz_{in}\right]\\&-\sum_k \dot{m}_{Gk}\left[e_{Gk}+\frac{p_{out}}{\rho_{Gk}}+\frac{1}{2}u_{Gk}^2+gz_{out}\right]-\sum_l \dot{m}_{Ll}\left[e_{Ll}+\frac{p_{out}}{\rho_{Ll}}+\frac{1}{2}u_{Ll}^2+gz_{out}\right]\end{aligned} \tag{4}$$

Atomization phenomena are an energy conversion process: the increment of the Laplace pressure and the surface free energy corresponds to the variance of the total amount of change in energy input, work output, energy source, total enthalpy, and potential energy. Eq.(4) can be simplified using following assumptions:

Assumption 1: There is no energy input and work output.
Assumption 2: No energy source is inside the control volume.
Assumption 3: The liquid/gas flow rates are conserved.
Assumption 4: Fluids are incompressible.
Assumption 5: The static pressure is constant.
Assumption 6: The potential energy is negligible.
Assumption 7: The physical properties are constant.
Assumption 8: The change in the internal energy is sufficiently smaller than that in the kinetic energy.

Implementing the above assumptions leads to Eq.(5):

$$\begin{aligned}&\sigma\left[\sum_l\left(\frac{2\dot{m}_{Ll}}{\rho_{Ll}\bar{R}_{Ll}}+\dot{S}_{Ll}\right)-\sum_j\left(\frac{2\dot{m}_{Lj}}{\rho_{Lj}\bar{R}_{Lj}}+\dot{S}_{Lj}\right)\right]\\&=\left(\sum_i\frac{1}{2}\dot{m}_{Gi}u_{Gi}^2-\sum_k\frac{1}{2}\dot{m}_{Gk}u_{Gk}^2\right)\\&+\left(\sum_j\frac{1}{2}\dot{m}_{Lj}u_{Lj}^2-\sum_l\frac{1}{2}\dot{m}_{Ll}u_{Ll}^2\right)\end{aligned} \tag{5}$$

It expresses that an increase in the Laplace pressure and the surface free energy corresponds to a decrement in the kinetic energy [21]. Atomization efficiency is defined as η_σ= (increase in Laplace pressure and surface free energy) / (inflow energy).

$$\eta_\sigma\equiv\frac{\sigma\left[\sum_l\left(\frac{2\dot{m}_{Ll}}{\rho_{Ll}\bar{R}_{Ll}}+\dot{S}_{Ll}\right)-\sum_j\left(\frac{2\dot{m}_{Lj}}{\rho_{Lj}\bar{R}_{Lj}}+\dot{S}_{Lj}\right)\right]}{\sum_i\frac{1}{2}\dot{m}_{Gi}u_{Gi}^2+\sum_j\frac{1}{2}\dot{m}_{Lj}u_{Lj}^2} \tag{6}$$

It also corresponds to the ratio of decrease in the kinetic energy to the inflow kinetic energy.

$$\eta_\sigma=\frac{\left(\sum_i\frac{1}{2}\dot{m}_{Gi}u_{Gi}^2-\sum_k\frac{1}{2}\dot{m}_{Gk}u_{Gk}^2\right)+\left(\sum_j\frac{1}{2}\dot{m}_{Lj}u_{Lj}^2-\sum_l\frac{1}{2}\dot{m}_{Ll}u_{Ll}^2\right)}{\sum_i\frac{1}{2}\dot{m}_{Gi}u_{Gi}^2+\sum_j\frac{1}{2}\dot{m}_{Lj}u_{Lj}^2}\,. \tag{7}$$

The maximum atomization efficiency, $\eta_{\sigma\max}$, is attained when the decrease in the kinetic energy is the maximum without any other energy losses. Finally, the assumption below is introduced:

Assumption 9: there is no inflow or outflow of gas.

Then, we obtain Eq.(8).

$$\sigma\left[\sum_l\left(\frac{2\dot{m}_{Ll}}{\rho_{Ll}\bar{R}_{Ll}}+\dot{S}_{Ll}\right)-\sum_j\left(\frac{2\dot{m}_{Lj}}{\rho_{Lj}\bar{R}_{Lj}}+\dot{S}_{Lj}\right)\right]=\eta_\sigma\sum_j\frac{1}{2}\dot{m}_{Lj}u_{Lj}^2 \tag{8}$$

DERIVATION OF SMD AND DISTRIBUTION

Based on the simplified equation of energy conservation law, we formulate SMD (d_{32}). The relationships between $\dot{m}$ and $\dot{S}$ are:

$$\text{Spherical droplet}: \quad \dot{S}=6\dot{m}/\rho d \tag{9}$$

Liquid column : $\dot{S} = 4\dot{m}/\rho D$. (10)

Considering the case that a liquid column comes into the control volume and spherical droplets go out, Eq.(11) is obtained by substituting Eqs.(9) and (10) into Eq.(8).

$$\sigma\left[\sum_{out}\left(\frac{2\dot{m}}{\rho\overline{R}}+\dot{S}\right)-\sum_{in}\left(\frac{2\dot{m}}{\rho\overline{R}}+\dot{S}\right)\right]=\frac{10\sigma}{\rho}\sum_{out}\frac{\dot{m}}{d}-\frac{6\sigma\dot{m}_L}{\rho D} \quad (11)$$
$$=\eta_\sigma\cdot\dot{k}_{in}$$

The sum of the Laplace pressure and the surface free energy of the droplets is proportional to $\sum_{out}(\dot{m}/d)$, which is expressed by Eq.(12) using a surface mean diameter d_{20}.

$$\sum_{out}\frac{\dot{m}}{d}=\dot{N}\times\left(\overline{\frac{1}{6}\rho\pi d^3/d}\right)=\dot{N}\times\frac{1}{6}\rho\pi d_{20}^2 \quad (12)$$

The total flow rate $\dot{m}_L$ is provided by Eq.(13) using a volume mean diameter d_{30}.

$$\dot{m}_L=\sum_{out}\dot{m}=\dot{N}\times\left(\overline{\frac{1}{6}\rho\pi d^3}\right)=\dot{N}\times\frac{1}{6}\rho\pi d_{30}^3 \quad (13)$$

Dividing Eq.(12) by Eq.(13), d_{32} is given.

$$\frac{1}{d_{32}}\equiv\frac{d_{20}^2}{d_{30}^3}=\frac{\sum_{out}\dot{m}/d}{\dot{m}_L}. \quad (14)$$

By substituting Eq.(14) into Eq.(11), the non-dimensional d_{32} is obtained.

$$\frac{d_{32}}{D}=\frac{20}{\eta_\sigma\dfrac{\dot{k}_{in}}{\dot{k}_{uni}}We+12} \quad (15)$$

Here, $\dot{k}_{uni}$ is the kinetic energy at the uniform injection, which given by $\dot{k}_{uni}=\pi\rho V_e^3D^2/8$.

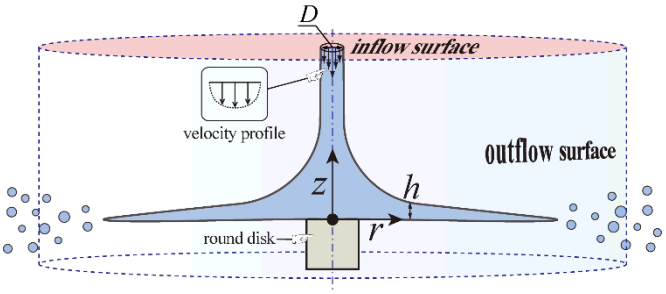

Fig. 2 Schematics of axisymmetric liquid sheet by jet impact and control volume

Figure 2 shows the present analysis model. A liquid jet impacts on a round disk and an axisymmetric liquid sheet expands. The coordinate system, (r, z), has its origin at the stagnation point on the disk. The inflow plane of the control volume is defined at the nozzle exit, and the outflow plane is set far downstream after the atomization has completed. As indicated in Eq.(15), SMD is calculated when the kinetic energy at the inlet/outlet, and the Weber number are provided. To specify the injection conditions, the jet is turbulent flow, whose injection velocity profile follows $1/n^{\text{th}}$-power law.

$$V=\frac{(n+1)(2n+1)}{2n^2}\left(1-\frac{2r}{D}\right)^{1/n}V_e \quad (16)$$

Injection velocity profiles have impacts on the atomization characteristics [22][23]. Following assumptions are added:

Assumption 10: No energy loss is incurred by the impact.

Assumption 11: The velocity inside the liquid sheet becomes uniform due to its viscosity [23].

Assumption 12: Atomization occurs after the internal velocity of the liquid sheet has become uniform.

Taking into account the above assumptions, a decrease in the kinetic energy is calculated. Hereafter, the properties without subscripts denote those of the liquid.

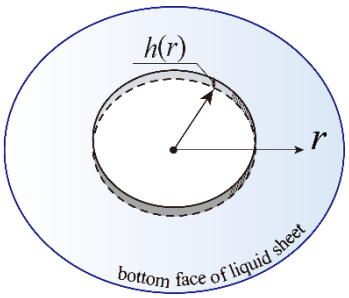

Fig. 3 Perspective view of the liquid sheet

Figure 3 shows the cross-sectional view of the liquid sheet. Between the liquid jet and the liquid sheet after the internal velocity has become uniform, the conservations of mass and momentum flow rate are given as follows.

Mass: $\frac{1}{4}\pi\rho D^2V_e=2\pi rh\rho u_\infty$ (17)

Momentum:

$$\frac{(n+1)(2n+1)^2}{16n^2(n+2)}\rho\pi D^2V_e^2=2\pi rh\rho u_\infty^2 \quad (18)$$

, where u_∞ is the velocity inside the liquid sheet after the uniformity has been established. From Eqs.(17) and (18), the velocity and thickness of the sheet are derived:

$$u_\infty=\frac{(n+1)(2n+1)^2}{4n^2(n+2)}V_e \quad (19)$$

$$h=\frac{n^2(n+2)}{2(n+1)(2n+1)^2}\frac{D^2}{r}. \quad (20)$$

We obtain the kinetic energy at the inlet and the outlet of the control volume.

$$\dot{k}_{in}=\frac{(n+1)^3(2n+1)^3}{32n^4(n+3)(2n+3)}\pi\rho D^2V_e^3 \quad (21)$$

$$\dot{k}_{out}=\frac{1}{2}u_\infty^2\rho u_\infty\cdot2\pi rh=\frac{(n+1)^2(2n+1)^4}{128n^4(n+2)^2}\pi\rho D^2V_e^3 \quad (22)$$

The kinetic energy decreases inside the control volume in the process of the velocity uniformity. The value of η_σ is given as:

$$\eta_\sigma=\frac{\dot{k}_{in}-\dot{k}_{out}}{\dot{k}_{in}}=\frac{5n+7}{4(n+1)(n+2)^2} \quad (23)$$

, which corresponds to η_σ=1.6% of the inlet kinetic energy at n=7. This value is independent of the injection velocity, nozzle diameter and physical properties.

By substituting Eq.(23), $\dot{k}_{in}$, and $\dot{k}_{uni}$ into Eq.(15), d_{32} is obtained as:

$$\frac{d_{32}}{D}=\frac{20}{\dfrac{(n+1)^2(2n+1)^3(5n+7)}{16n^4(n+2)^2(n+3)(2n+3)}We+12}. \quad (24)$$

Under the condition of n=7, d_{32} is given as follows.

$$\frac{d_{32}}{D} = \frac{10}{50We/5831+6} \tag{25}$$

At We>>10^3, d_{32} is inversely proportional to the Weber number.

$$\frac{d_{32}}{D} = \frac{5831}{5We} \approx \frac{1000}{We} \tag{26}$$

When the jet is very slow (We<<1), we obtain d_{32}/D=1.67 from Eq.(15), which corresponds to the Rayleigh criteria of $d/D=(3\pi/2)^{1/3}$=1.68 [24].

In the present analysis, exponential distribution is simply presumed as a droplet size distribution.

$$f_N(d) = \lambda \exp(-\lambda d) \tag{27}$$

A normalized formulation using d_{32} is

$$d_{32} \cdot f_N(d) = 3\exp(-3d/d_{32}) \tag{28}$$

or

$$\frac{5831D}{5We} \cdot f_N(d) = 3\exp(-\frac{15We}{5831}\frac{d}{D}). \tag{29}$$

Formulated other mean diameters are summarized in Table 1.

Table 1 Theoretical mean diameters

mean diameters	theory
d_{10}/D	$\frac{5}{75We/5831+9}$
d_{20}/D	$\frac{5\sqrt{2}}{75We/5831+9}$
d_{30}/D	$\frac{5\sqrt[3]{6}}{75We/5831+9}$
d_{32}/D	$\frac{5}{25We/5831+3}$

VALIDATION OF THE THEORETICAL METHOD

To validate the proposed estimation framework, droplet diameters are experimentally measured under the condition of practical use of We>1000.

Experimental Apparatus and Conditions

Figure 4(a) shows an experimental apparatus. A working liquid, water, is pressurized in a reservoir, and is injected into still air through a precision glass tube, whose diameter is of 1.4mm, 2.0mm and 2.6mm, and straight length of 30mm. A liquid jet impinges on the center of a round disk (6.35mm in dia.) located 5mm downstream and a liquid sheet spreads (see Fig.4(b)). Table 2 shows the physical properties of working fluids. The surface tension coefficient is measured by the Wilhelmy plate method utilizing automatic surface tensiometer (Kyowa CBVP-Z). Double pulse YAG Laser (DANTEC DYNAMICS DualPower 135-15) is used for the background light. A long distance microscopic lens (INFINITY Model K2/SC) enlarges the area of 4mm×4mm at the side of the impact point of 150mm. The shadow images of droplets in the region are taken by a CCD camera (DANTEC DYNAMICS FlowSense 4M MkII). Space resolution is 2μm/pixel. More than ten thousand of droplets are analyzed to measure their diameter and velocity. The experimental results are based on the number of droplets per unit time passing through the outflow surface of the control volume corresponding to the theoretical analysis. We confirmed the axis-symmetry of droplet diameters, and the convergence both of mean diameters and size distributions. Present measurement results, therefore, are representative values of all of the spreading droplets. Table 3 shows typical injection conditions. Liquid jets are injected subject to fully developed turbulent conditions. From the mass of outflow in a period of time, injection velocity is calculated. Cavitation inside the nozzle is not observed.

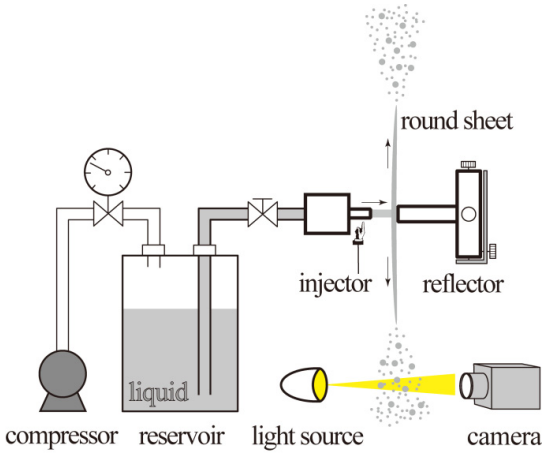

(a) Schematics of apparatus

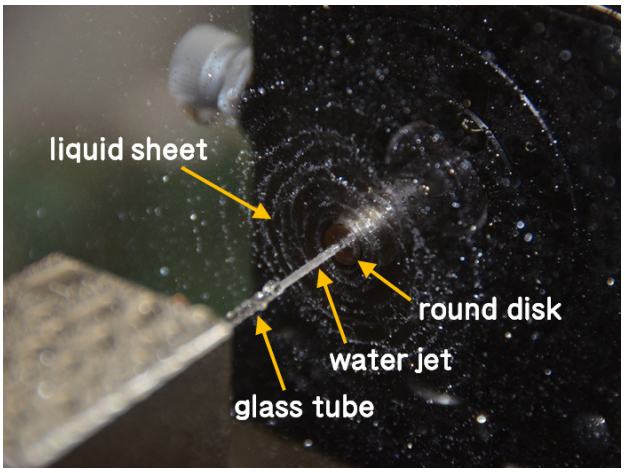

(b) Liquid jet and sheet
(The round disk is attached to a fine movement apparatus.)

Fig.4 Experimental setup

Table 2 Physical properties of working fluids

fluid	ρ [kg/m^3]	μ [Pa·s]	σ [mN/m]
air	1.2	1.8×10^{-5}	72.4±0.4
water	1000	1.0×10^{-3}	

Table 3 Injection conditions

D [mm]	V_e [m/s]	We	Re
1.4, 2.0, 2.6	5~20	1000~20000	>10^4

Results of Theory and Experiment

Figure 5 shows experimental results of d_{32}/D at various injection Weber number and a calculated result of Eq.(25). Experimental results of d_{32}/D are independent of the nozzle diameter and gradually decrease as increment of *We*. At *We* > 4000, they become a constant value of d_{32}/D=0.15, where an interaction between liquid and surrounding gas becomes dominant. The theoretical result linearly decreases inversely proportional to *We* and represents experimental values at the accuracy of 0.5~2 times of them. Table 4 indicates other mean diameters formulated in Table 1 also have the same degree of accuracy.

Figure 6 shows results of non-dimensional size distributions. At *We*=2400~12000 (Fig.6(a)), experimental results converge. The theoretical result of Eq.(28) captures the trend of experimental results of large droplets. Since the distribution function becomes 3 at small d/d_{32}, the distributions of small droplets are not reproduced. At *We*=1300 (Fig.6(b)), the discrepancy is large, where the force balance of inertia and surface tension at the edge of the sheet determines the sizes.

The proposed framework in general is shown to be valid enough as long as a tool for the order estimation technique. Strictly speaking, the situation, where all the assumptions are accurately regarded to be correct, is quite limited. Progression of the estimation method will be achieved by applying more practical assumptions and boundary conditions.

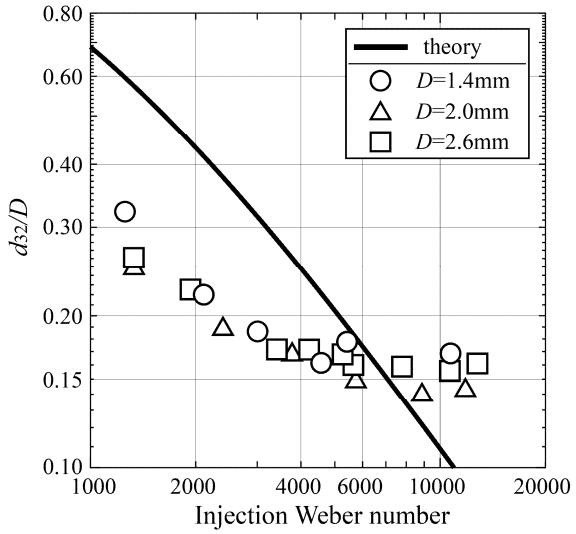

Fig.5 Experimental and theoretical results of SMD

Table 4 Comparison of several mean diameters

	theory/exp.		
We	d_{10}	d_{20}	d_{32}
2400	1.4	1.7	2.0
5700	1.0	1.1	1.2
12000	0.52	0.59	0.65

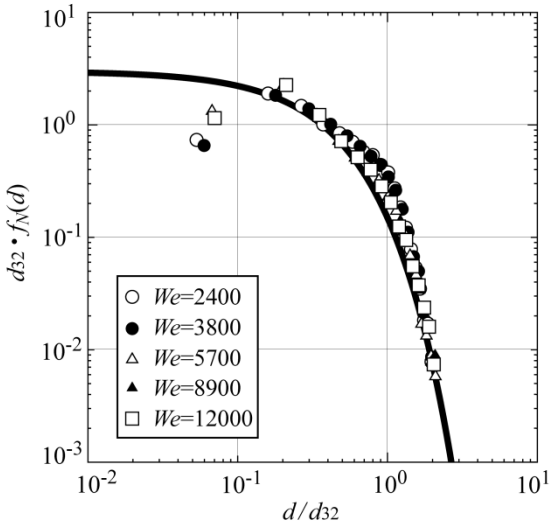

(a) *We*=2400~12000

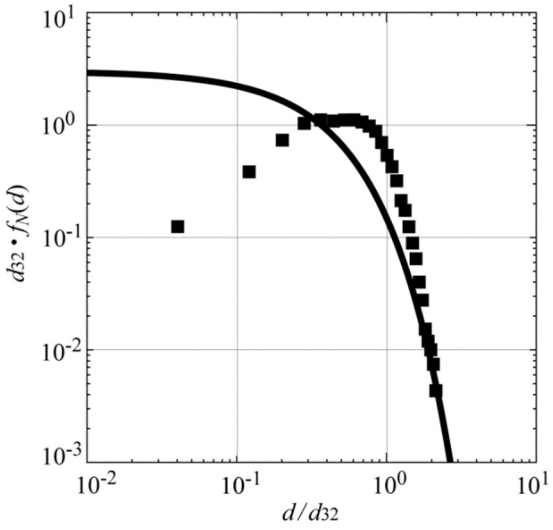

(b) *We*=1300

Fig. 6 Non-dimensional drop size distribution with exponential distribution (bold line)

(*D*=2mm, Experimental $d_{32}\cdot f_N(d)$ corresponds to $d_{32}\cdot n_i/(\Sigma n_i\cdot \triangle d)$, where n_i means the number of drops within the diameter of d_i-$\triangle d$ /2<d_i< d_i+$\triangle d$ /2. Here,$\triangle d$=40μm.)

ENERGY CONVERSION PROCESS

In the theoretical framework, the atomization is induced by decrement of kinetic energy through the velocity uniformity process inside the sheet. We demonstrate the uniformity process by conducting a numerical simulation. The governing equations are three-dimensional Navier-Stokes equations for the free surface flow and an equation of motion for discrete droplets. Solving the them, Eulerian and Lagrangian hybrid scheme is employed: Continuous liquid surface is tracked by PLIC-VOF scheme and spreading droplets are seamlessly converted to mass points. Detailed method is described in [18]. Figure 7 shows a numerical result. The injected liquid jet with 1/7 power-law velocity profile impacts on a round disk as in the experimental setup and the sheet spreads. From the edge of the sheet, droplets are produced. To investigate the flow inside the sheet, the jet is

perpendicularly injected to a slip wall. Figure 8 shows developing velocity profile inside the sheet. At close to the stagnation point, r=1D, the radial velocity is not uniform. The distribution gradually becomes uniform, and a uniform profile realizes at r=7D. Through this process, the injected kinetic energy is eventually converted to the surface free energy, which causes atomization in Fig.7.

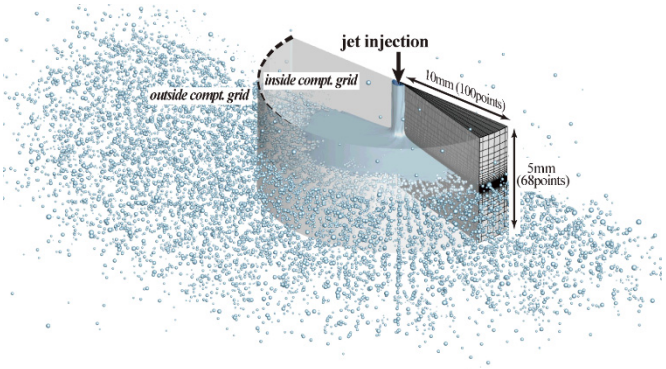

Fig. 7 Result of simulation.
(Half of the axisymmetric liquid sheet is shown.)

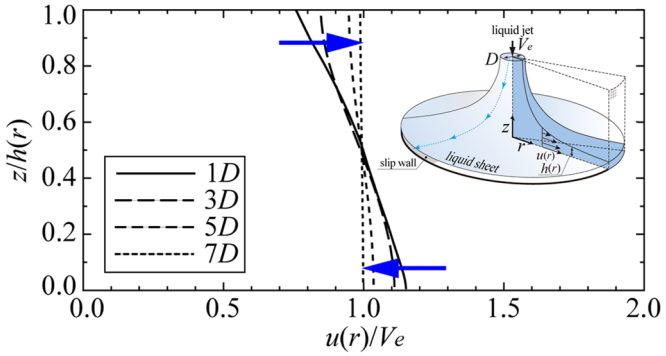

Fig. 8 Uniformity process of radial velocity inside liquid sheet.
(Result of numerical simulation. $z/h(r)$=0.0 and $z/h(r)$=1.0 correspond to the location of slip wall and that of liquid/gas free surface, respectively.)

CONCLUSIONS

Based on the energy conservation law, a framework of the consistent analytical model was proposed and validated for calculating droplet diameters and size distributions produced by liquid sheet atomization. Conclusions are summarized as follows.

(1)Under several hypotheses, e.g. ignoring effects of ambient gas, the increase in the Laplace pressure and the surface free energy is equal to the decrease in the kinetic energy. The droplet diameter can be calculated when the amount of kinetic energy loss is reasonably estimated.

(2)In the case of turbulent flow injection assuming a 1/7 power law, 1.6% of the inlet kinetic energy decreases through the velocity uniformity process inside the sheet.

(3)The proposed estimation method is able to calculate the SMD without using any experimental parameters. The theoretical results reproduced the order of magnitude of the corresponding experimental results.

(4)Non-dimensional exponential distribution function using the formulated SMD reproduced the experimental results at We>2000.

(5)A numerical simulation confirmed the velocity uniformity process inside the sheet.

The next step is to extended the theoretical framework applicable to atomization with co-flowing gas stream.

NOMENCLATURE

$\dot{C}$	:	energy source	[J/s]
d	:	droplet diameter	[m]
d_{10}	:	arithmetic mean diameter	[m]
d_{32}	:	Sauter mean diameter (SMD)	[m]
D	:	nozzle diameter	[m]
e	:	internal energy	[J/kg]
$f_N(d)$	:	number of probability density function	[1/m]
g	:	gravity acceleration	[m/s^2]
h	:	liquid sheet thickness	[m]
$\dot{k}$	:	kinetic energy flux	[J/s]
$\dot{m}$	:	mass flow rate	[kg/s]
$\dot{m}_L$	:	total mass flow rate from a nozzle	[kg/s]
$\dot{N}$	:	rate of droplet production	[1/s]
p	:	static pressure	[Pa]
$\dot{Q}$	:	heat flux	[J/s]
r	:	radial distance	[m]
$1/\overline{R}$	:	averaged curvature	[1/m]
Re	:	Reynolds number($\rho V_e D/\mu$)	[-]
$\dot{S}$	:	liquid surface area, A[m^2], through a specific plane per unit time($\delta A/\delta t$).	[m^2/s]
u	:	radial velocity	[m/s]
V	:	injection velocity	[m/s]
V_e	:	averaged velocity	[m/s]
$\dot{W}$	:	work	[J/s]
We	:	Weber number($\rho V_e^2 D/\sigma$)	[-]
λ	:	parameter of exponential distribution function	[1/m]
μ	:	coefficient of viscosity	[Pa･s]
ρ	:	density	[kg/m^3]
σ	:	surface tension coefficient	[N/m]
η_σ	:	atomization efficiency	[-]

Subscripts

G / L	:	gas / liquid
i,j,k,l	:	number of each jet/drop
in/out	:	inlet/outlet

REFERENCES

[1] Ashgriz,N.: Spray Nozzles, Handbook of Atomization and Sprays(Springer), Chapter24(2011), pp.497-579.

[2] Liu,H.: Science and Engineering of Droplets: Fundamentals and Applications (Materials Science and Process Technology)(William Andrew)(2000).

[3] Fraser,R.P., Eisenklam,P., Dombrowski,N., and Hasson,D.: Drop Formation from Rapidly Moving

Liquid Sheets, A.I.Ch.E. Journal, Vol.8, No.5(1962), pp.672-680.
[4] Inamura,T., Daikoku,M., Kumakawa,A., and Tamura,H.: Numerical Prediction of Spray Characteristics Produced by Like-Doublet Impinging Jets, Proceedings of 15th Atomization Symposium (2006), pp.147-152.
[5] Dechelette,A., Babinsky,E. and Sojka,P.E.: Drop Size Distributions, Handbook of Atomization and Sprays(Springer), Chapter23(2011), pp.479-495.
[6] Babinsky,E. and Sojka,P.E.: Modeling drop size distributions, Progress in Energy and Combustion Science, Vol.28(2002), pp.303-329.
[7] ILASS-Japan: Atomization Technology, Morikita-Shuppan(2001).
[8] Sellens,R.W. and Brzustowski,T.A.: A prediction of drop-size distribution in a spray from first principles, Atomization Spray Technology, Vol.1(1985), pp.89-102.
[9] Li,X. and Li,M.: Droplet Size Distribution in Sprays Based on Maximization of Entropy Generation, Entropy, Vol.5(2003), pp.417-431.
[10] Sovani,S.D. and Sojka,P.E., and Sivathanu,Y.R.: Prediction of Drop Size Distributions from First Principles: The influence of Fluctuations in Relative Velocity and Liquid Physical Properties, Atomization and Sprays, 9(1999), pp.113-152
[11] Sovani,S.D. and Sojka,P.E., and Sivathanu,Y.R.: Prediction of Drop Size Distributions from First Principles: Joint-PDF Effects, Atomization and Sprays, 10(2000), pp.587-602
[12] Apte,S.V., Gorokhovski,M., and Moin,P.: LES of atomizing spray with stochastic modeling of secondary breakup, International Journal of Multiphase Flow, 29(2003), pp.1503–1522.
[13] Gorokhovski,M., and Herrmann,M.: Modeling Primary Atomization, Annual Review of Fluid Mechanics, 40(2008), pp.343–366.
[14] Menard,T., Tanguy,S., and Berlemont, A.: Coupling level set/VOF/ghost fluid methods: Validation and application to 3D simulation of the primary break-up of a liquid jet, International Journal of Multiphase Flow, 33(2007), pp.510–524.
[15] Shinjo,J. and Umemura,A.: Detailed simulation of primary atomization mechanisms in Diesel jet sprays (isolated identification of liquid jet tip effects), Proceedings of the Combustion Institute, 33(2011), pp. 2089–2097.
[16] Herrmann,M.: Detailed Numerical Simulations of the Primary Atomization of a Turbulent Liquid Jet in Crossflow, Journal of Engineering for Gas Turbines and Power 132(2010), 061506.
[17] Arienti,M., Li,X., Soteriou,M.C., Eckett,C.A., and Jensen,R.: Coupled Level-Set/Volume-Of-Fluid Method for The Simulation of Liquid Atomization in Propulsion Device Injectors, AIAA 2010-7136, 46th AIAA/ASME/SAE/ASEE Joint Propulsion Conference & Exhibit, 25 - 28 July 2010, Nashville, TN.
[18] Inoue,C, Shimizu,A, Watanabe,T, Himeno,T, and Uzawa,S.: Numerical and Experimental Investigation on Spray Flux Distribution Produced by Liquid Sheet Atomization, Proceedings of ASME Turbo Expo 2015, GT2015-43364, pp.1-10 (2015).
[19] Inoue,C, Watanabe,T, Himeno,T, and Koshi,M.: Consistent Estimation Method of Spray Diameter and Size Distribution Based on Energy Conservation Law, *Trans. JSME, Ser.B*, 78(2012), pp.850-861(in Japanese).
[20] Inoue,C, Watanabe,T, Himeno,T, Uzawa,S. and Koshi,M.: Consistent Theoretical Model of Mean Diameter and Size Distribution by Liquid Sheet Atomization, Proceedings of ASME Turbo Expo 2012, GT2012-70087, pp.1-10 (2012).
[21] Sato,H.: Study on Disintegration Mechanism of Liquids, Proceedings of ICLASS-'97(1997), pp.46-53.
[22] McCarthy,M.J. and Molloy,N.A.: Review of Stability of Liquid Jets and the Influence of Nozzle Design, The Chemical Engineering Journal, 7(1974), pp.1-20.
[23] Inoue,C., Watanabe,T., and Himeno,T.: Atomization and Flow Characteristics of Liquid Sheet Produced by Jet Impingement, Journal of Propulsion And Power, 28(2012), pp.1060-1070.
[24] Rayleigh,L : On the Instability of Jets, Proceedings of the London Mathematical Society. Ser. 1 Vol.10(1878), pp.4-13.